

# *Study on dynamic-microphysical-electrical processes in severe thunderstorms and lightning hazards (STORM973)*

*Xiushu Qie, Gaopeng Lu, Dongxia Liu, Rubin Jiang*  
Key Laboratory of Middle Atmosphere and Global  
Environment Observation (LAGEO), Institute of  
Atmospheric Physics, CAS, Beijing, China, 100029  
qiex@mail.iap.ac.cn

*Yijun Zhang and Weitao Lu*  
Laboratory of Lightning Physics and Protection  
Engineering, Chinese Academy of Meteorological  
Sciences, Beijing 100081, China

*Qilin Zhang and Yan Yin*  
Key Laboratory for Aerosol-Cloud-Precipitation of China  
Meteorological Administration, Nanjing University of  
Information Science and Technology,  
Nanjing 210044, China

*Debin Su*  
Institute of Urban Meteorology,  
China Meteorological Administration,  
Beijing Meteorological Service,  
Beijing 100089, China

**Abstract**—A coordinated research effort across China has been undertaken to study the dynamic-microphysical-electrical processes in severe thunderstorms and lightning hazards funded as National Key Basic Research Program (Storm973, 2014-2018) by the Ministry of Science and Technology of China. The Storm973 project is desired to 1) establish a comprehensive observational dataset of severe thunderstorms in northern China; 2) reveal the interaction between dynamic, microphysical, and electrical processes in severe thunderstorms and the associated mechanism; 3) clarify the physical mechanism of lightning occurrence and development, effect of electromagnetic radiation, and hazard causes; 4) achieve the parameterization of lightning in numerical models, the assimilation and application of lightning data, and the forecasting and early warning for severe thunderstorms and lightning hazards. This review talk will cover the major research advances related to this program in the first two years of 2014 and 2015.

**Keywords**—lightning; thunderstorm; detection; physical mechanism; lightning assimilation

## I. INTRODUCTION

Severe thunderstorms usually produce lightning, rainfall, wind, hail, and possibly tornado. They are major precipitation processes and often lead to flooding and disastrous consequences in China. Lightning, the defining process of thunderstorms, is also a major threat for the general public and affects the normal operation of many national infrastructures and public utilities. In China, lightning injures or kills over a

thousand people and costs 7-10 billion Chinese Yuans (1-2 billion US dollars) in property losses annually. There is an urgent need to improve our understanding of lightning and thunderstorms in order to prevent or mitigate their detrimental effects. A coordinated research effort across China has been undertaken to study the dynamic-microphysical-electrical processes in severe thunderstorms and lightning hazards funded as National Key Basic Research Program (Storm973, 2014-2018) by the Ministry of Science and Technology of China.

Storm973 Project will carry out six major research subjects, including 1) Comprehensive integration of detection systems for thunderstorm and coordinated observations; 2) Dynamic processes and evolution of severe thunderstorms; 3) Cloud microphysical processes and their effects on electrical structure in severe thunderstorms; 4) Incloud charge distribution and mechanism of lightning initiation and propagation in severe thunderstorms; 5) Physical processes of lightning development and hazard causes; and 6) Data assimilation of special observations, forecast and early warning methods of severe thunderstorms and lightning hazards. This review talk covers some major research advances in lightning detection, lightning meteorology, and lightning physics related to this program in the first two years of 2014 and 2015.

## II. COORDINATED OBSERVATIONS

During Storm973 Project, the field campaigns is scheduled to be carried out in Beijing, Shandong, and Guangdong for different scientific objectives from 2014-2018. The Beijing campaign aims to establish a comprehensive observational dataset and reveal the interaction between dynamic, microphysical, and electrical processes for severe thunderstorms, while Shandong and Guangzhou campaigns mainly focus on lightning physics and effects.

### A. Coordinated observations on thunderstorm in Beijing-Tianjin-Langfang city cluster area

To detect severe thunderstorms around Beijing, two X-band multi-parameter radar and Beijing Lightning Network (BLNet) have been utilized in Storm973. The campaign also integrates with the meteorological operational networks of S-band Doppler radar, cloud-to-ground (CG) lightning, rain gauge and automatic meteorological station.

The BLNET is a regional multi-frequency-band lightning detection network and has been developed for both research and operational purposes (Wang et al., 2016). The network consisted of 16 stations in 2015 covering most part of the “Jing-Jin-Ji” (Beijing-Tianjin-Hebei) metropolis zone, one of the most developed areas in China. Fig. 1 shows a layout of E-field sensors of BLNet. Four different sensors, including slow antenna, fast antenna, magnetic antenna, and VHF antenna, covering a bandwidth from VLF to VHF, are integrated in each station to detect lightning radiation signals in different frequency band. The Chan algorithm and Levenberg-Marquardt method are adopted jointly in the lightning location algorithm. In addition to locate the lightning radiation pulses in 2D or 3D in different band, the charge source neutralized by the lightning discharge can be retrieved either. The theoretical horizontal error over the network is less than 200 m and the vertical error is less than 500 m over the network. The comparison of total lightning location results with corresponding radar echoes for thunderstorm cases indicates good performance of BLNET in severe convection surveillance.

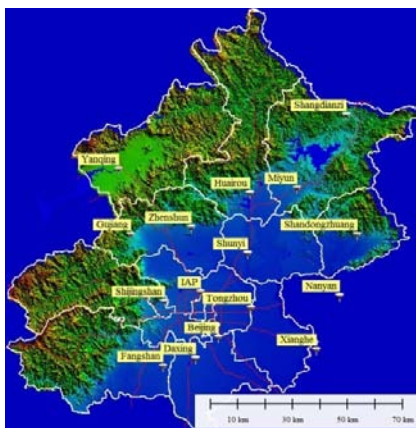


Fig. 1. Layout of E-field sensors of BLNet.

The BLNet are expected to realize the following functions: (1) to locate both intracloud (IC) lightning and lightning radiation pulses in 2D in real time for severe thunderstorm warning, (2) to map IC and CG lightning discharge in 3D for

research, (3) to document electromagnetic waveform and analyze its characteristics, and (4) to determine charge sources neutralized by lightning processes.

The thunderstorm detection field campaign of Storm973 has been conducted in 2014-2015, and will be continued in the following 3 years. A total of 80 thunderstorm events were documented through the last two-year observation. Although a wide variety of storm types were observed during the campaign, it is found that two major convective weather system, squall line and  $\gamma$ -meso scale thunderstorm group, are two major kinds of convective weather systems intriguing Beijing with damages or unexpected local heavy rain and lightning.

### B. Rocket-triggering lightning experiment

In order to get new insights into the lightning physical process and its electromagnetic effects in the close environment, rocket-triggering lightning experiments are conducted in two sites, Zhanhua, Shandong Province (SHATLE) and Conghua, Guangdong Province (GCOELD), respectively. Fig. 2 and Fig. 3 show the installation of rocket-triggering lightning experiment in both sites. The following instruments are effectively integrated during the experiment, including short-baseline 2D VHF/UHF Lightning Mapping Interferometer (LMI), slow/fast antenna, high-speed video cameras and optical measurements with a photodiode array, LF magnetic sensors, and so on. In GCOELD, the new testing system of lightning hazards has been constructed with a dedicated goal to study the mechanism of damages to power transmission lines (both in air and buried underground) and lightning protection devices.



Fig. 2. Installation of rocket-triggering lightning experiment in Zhanhua, Shandong (SHATLE).



Fig. 3. Installation of rocket-triggering lightning experiment in Conghua, Guangdong (GCOELD).

### C. Tall-object lightning observatory in Guangzhou

To study the process of lightning flashes striking tall structures, a field experiment is conducted in Guangzhou, Guangdong Province, China, a metropolis that contains many tall structures. The Tall-Object Lightning Observatory in Guangzhou (TOLOG) has been established (Lu et al., 2013). Two observation stations are involved in the experiment. The main observation station is located on a  $\sim 100$  m building that belongs to the Guangdong Meteorological Bureau, and the sub-station is located on a  $\sim 70$  m building. The positions of the observation stations and the tallest structures are presented in Fig. 1. The FOV of the sub-station's optical observation system also covers the tallest structures.



Fig. 4. Tall-Object Lightning Observatory in Guangzhou (TOLOG).

## III. DYNAMIC-MICROPHYSICAL-ELECTRICAL PROCESSES AND EVOLUTION IN SEVERE THUNDERSTORMS

### A. Lightning characteristics related to radar morphology in linear convective systems

Utilizing data from the observation and archived data earlier, a total of 89 linear mesoscale convective systems (MCSs) that occurred in Beijing-Tianjin-Langfang city cluster area are classified into six categories according to radar morphology: leading convective lines with a trailing stratiform region (TS), leading stratiform region with a trailing convective region (LS), leading convective lines with no stratiform region (NS), bow echo of leading lines (BE), leading convective lines with a parallel stratiform region (PS), and break line stratiform (BL). TS-, LS- and PS-type accounted for 73% of all the linear MCSs. Lightning is located mainly in the strong radar echo of TS, LS, and PS modes at their mature stage. However, at the dissipating stage, the lightning gradually increases in the stratiform region of the TS type, whereas no lightning occur in the stratiform region of the LS mode, and +CG lightning accounts for a large percentage in linear MCS of PS.

### B. Numerical simulation on effect of dynamic and microphysical processes on electrification inside thundercloud

Two electric-coupled thunderstorm models are developed based on mesoscale model of RAMS and WRF. Liu et al., (2014) introduced two noninductive electrification schemes, Takahashi78 (Takahashi, 1978) and Saunders98 (Saunders et al., 1998), and lightning discharge parameterization into the RAMSV6.0 model, and found that the simulated thunderstorm

shows a tripole charge structure under the Takahashi78 electrification scheme and changed from a dipolar to tripolar charge structure under the Saunders98 scheme. The simulated lightning frequency was consistent with observation. The WRF-Electric model was developed by Xu et al. (2016), and four different charge separation schemes are introduced into two microphysics schemes in WRF. The simulation confirms a dynamical-derived mechanism of inverted charge structure formation. The charging processes between the two particles mainly occurred at the top of the cloud where the graupel charged negatively and ice crystals positively due to the strong updraft. When the updraft air reached the top of the storm, it would spread to the rear and front. The light ice crystals were transported backward and forward more easily. Meanwhile, the positively charged ice crystals were transported downward by the frontal subsidence, and then a positive charge region formed between the  $-10^{\circ}$  C and  $-25^{\circ}$  C levels. Subsequently, a negative charge region materialized in the upper level of the cloud, and the inverted charge structure formed.

Wang et al.(2015a, b) examined the impact of the vertical velocity field on charging processes and charge separation in a simulated thunderstorm, and it is found that the ice particles in the vertical velocity range from 1 to 5 m/s obtained the most charge through charging processes during the lifetime of the thunderstorm. The vertical velocity conditions in the quasi-steady region (updraft speed between -1 and 1 m/s) were the most conducive for charge separation on different scales. Accordingly, a net charge structure always appeared in the quasi-steady and adjacent regions.

Zhao et al. (2014) investigated the effects of aerosol on electrification of an idealized supercell storm using the WRF model coupled with electrification and discharge parameterizations and an explicit treatment of aerosol activation. It is found that the microphysical and electric processes of the thunderstorm are distinctly different under different aerosol background. Enhancing aerosol loading increases growth rate of snow and graupel particles, and leads to higher concentration of ice particles, resulting in enhancement in electrification process.

### C. Effect of charge region in thunderstorms on lightning type

Tan et al. (2014a) investigated quantitatively the effect of lower positive charge (LPC) on lightning types using a 2D fine-resolution lightning discharge simulation. It is found that the LPC plays a key role in generating -CG flashes and inverted -IC lightning. With the increase of charge density or distribution range of LPC region, lightning type changes from positive polarity IC lightning to negative CG flashes and then to inverted IC lightning. Relative to distribution range of charge regions, the magnitude of charge density of the LPC region plays a dominant role in lightning type. Only when the maximal charge density value of LPC region is within a certain range, can negative CG flashes occur, and the occurrence probability is relatively fixed. Tan et al. (2014b) also found that potential at initiation point is a key to decide whether downward leader reaches ground. The absolute values of initiation potential of CG flashes are greater than 30 MV, while the absolute values of initiation potential of IC lightning are basically less than 30 MV. Since potential field is determined

by space charge distributions, polarities and types of lightning discharges are also dependent on relative locations and magnitudes of positive and negative charge zones near initiation points.

#### IV. OPERATIONAL APPLICATIONS OF LIGHTNING DATA AND LIGHTNING

##### A. Lightning data assimilation technique and application

Lightning data assimilation techniques are proposed and applied to improve the forecasts of convection and precipitation of thunderstorms. Yang et al. (2014) converted CG lightning data into 3D lightning-proxy radar reflectivity to adjust model variables (i.e., vertical velocity, specific humidity and specific cloud water content), based on a simply assumed relationship between flash density and reflectivity in the Grid point Statistical Interpolation (GSI) system. The results show that convection forecasting is improved with assimilation of the lightning-proxy reflectivity using the physical initialization method. There is significant improvement in the prediction of reflectivity, and this is maintained for about 3 h. Assimilating multi-time lightning data with assimilation cycles can further improve forecasting accuracy. Qie et al. (2014) established empirical relations between total lightning flash rate and the ice particle (graupel, ice, and snow) mixing ratio. The constructed nudging functions were used in the WRF model, and they found that the representation of convection was significantly improved one hour after the total lightning data assimilation, even during the assimilation period. The precipitation center, amount and coverage were all much closer to the observation in the sensitivity run with lightning data assimilation than in the control run without lightning data assimilation (refer to Fig. 5).

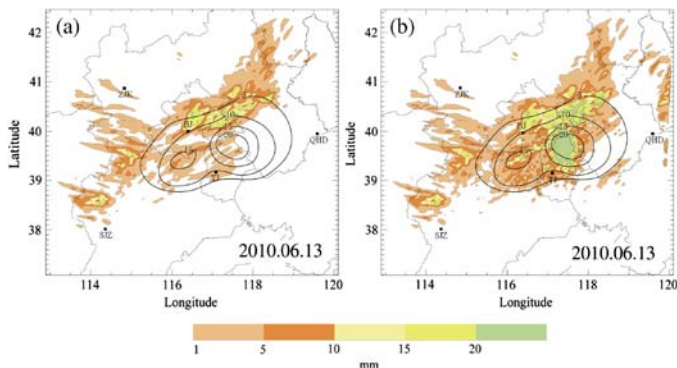


Fig. 5. Observed and forecasted total 6-hour precipitation (mm) from 20:00 on 13 June 2010: (a) control test without lightning assimilation; (b) sensitivity test with total-lightning assimilation. The black contours represent the observed precipitation from rain gauge data. The shaded areas indicate the simulated precipitation. [Adopted from Qie et al., 2014]

##### B. Lightning forecasting

Short-term lightning forecasting technique is being developed based on WRF model, and 2-6 hour forecasting period is expected. Meanwhile, Li et al. (2016) modified the lightning potential index proposed by Yair et al. (2010), and forecasted the occurrence of lightning by using the observed lightning data. The forecasting is tested for a quasi-linear MCSs in northern China based on the WRF model and the 3D-Var analysis system of the ARPS model. The lightning density

is calculated using both the precipitation and non-precipitation ice mass in the new method. It is found that most lightning activity is initiated on the right side and at the front of the MCSs, where the surface wind field converges intensely. The CAPE is much stronger ahead of the southeastward progressing MCS than to the back it, and their lightning events mainly occur in regions with a large gradient of CAPE.

#### V. PHYSICAL PROCESSES OF LIGHTNING DEVELOPMENT AND HAZARD CAUSES

##### A. New insight into leader propagation

With the high-quality data obtained during the rocket triggering lightning experiments in 2014-2015, many details involved in the 3D evolution of rocket-triggered lightning, natural CG lightning, and upward lightning from high buildings are revealed [Jiang et al., 2014; Lu et al., 2014; Gao et al., 2014; Sun et al., 2014, 2016].

Bidirectional development of dart leader propagating through pre-existing channel was observed in a high structure-initiated upward negative flash with high-speed camera [Jiang et al., 2014]. The dart leader initially propagated downward through the upper channel with decreasing speed and luminosity, and terminated in the air. It restarted subsequently its development at the terminated position with both upward and downward channel extensions. Fig. 6 shows propagation of the dart leader reproduced from the high speed camera images. The average 2D speed of upward positive end was  $5.3 \times 10^6$  m/s, while that of the downward negative end was  $2.2 \times 10^6$  m/s. The similar feature has been identified recently for the subsequent dart leader in rocket-triggered lightning.

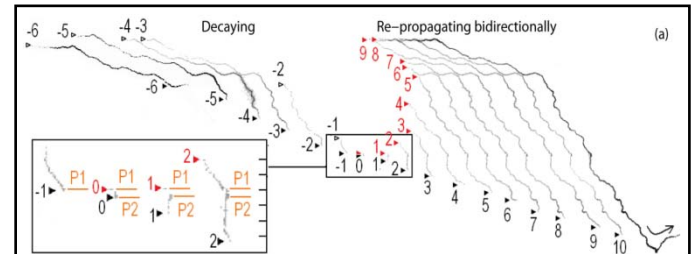


Fig. 6. Propagation of the dart leader reproduced from the high speed camera images. The frame number of "0" indicates the termination of the decaying downward leader and then the restart of the leader with bidirectional development. (Adopted from Jiang et al., 2014)

A short-baseline 2D VHF/UHF Lightning Mapping Interferometer (LMI) system is improved and employed to locate lightning broadband VHF radiation sources [Sun et al., 2014]. The system operating in a continuous mode is capable of capturing weak lightning signals, like positive upward leaders, and the discharge channel is mapped clearly (Fig. 7). For a rocket triggered lightning with 16 leader-return stroke sequences, the LMI-based speeds of upward positive leader was about  $10^4$  m/s, that of dart leaders were mostly of the order of  $10^6$ - $10^7$  m/s (with one exception of  $3.9 \times 10^5$  m/s for the 9th stroke), and that of dart-stepped leaders was of  $10^5$  m/s. It's also found that the chaotic pulse trains (CPTs) only occurred in the dart leader stage which propagated with a speed in an order of  $10^7$  m/s (Sun et al., 2016).

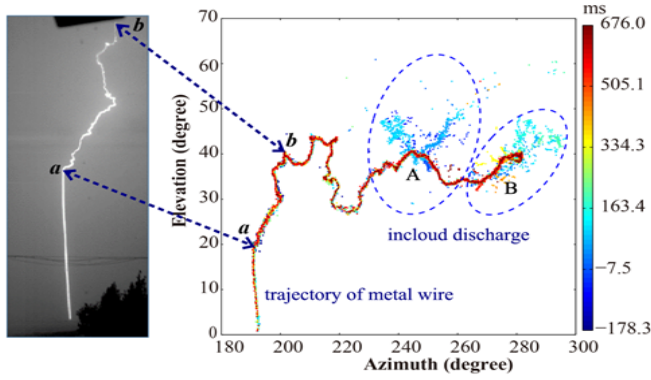


Fig. 7. Comparison of a rocket-triggered lightning flash mapped by the independent short-baseline 2D VHF/UHF Lightning Mapping Interferometer (LMI) system (right) and one frame from high-speed video images (left) [Adopted from Sun et al., 2014]

The propagation of upward positive leader was shown to be associated with a burst of electromagnetic pulses when it enters the negative charge region at the cloud base [Lu et al., 2014], which may suggest that the propagation of positive leader follows a stepped pattern. It is interesting to see that while the propagation of positive leader is active in radiating low-frequency magnetic pulses, it is relatively quite in the VHF band, implying that the stepping progression of positive leader might experience a fundamental change in the associated mechanism.

### B. New insight into connecting processes

Jiang et al. (2015) analyzed the grounding process and the associated leader behavior by using high-speed video record and time-correlated electric field change. For stepped leader-first return strokes, the upward connecting leaders tend to be induced by those downward leader branches with brighter luminosity and lower channel tip above ground, and they may accomplish the attachment with great possibility. The junction height of the dart leader with speed of higher than  $10^7$  m/s generates chaotic electric pulse trains, exhibits high junction height up to hundreds of meters (Fig. 8), and results in intense return stroke, which is quite different from the normal dart leader with short junction height in the order of meters (Jiang et al., 2015).

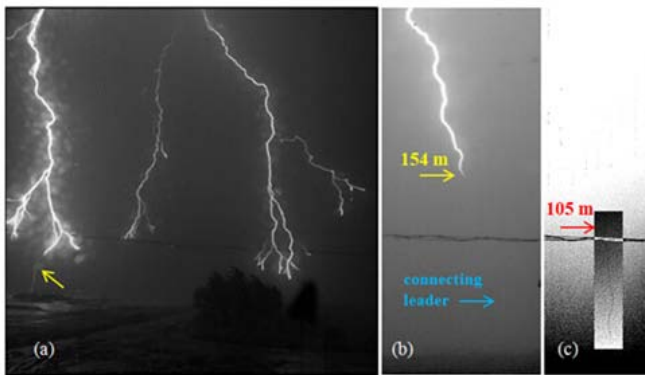


Fig. 8. Images of attachment processes for first and subsequent return strokes in natural lightning (Figure c is a regional contrast-modified image of Figure b, with the color-reversed connecting leader of subsequent return stroke) [Adopted from Jiang et al., 2015]

More details on the propagation of upward connecting leaders from high buildings in Guangzhou are obtained through the observation with respect to six negative CG flashes striking tall buildings from two separated high-speed video cameras [Gao et al., 2014], indicating that the 3-D velocity is typically 30% higher than the 2-D velocity as determined from the video observation at one site (Fig. 9). Also, the dynamic behavior of upward leader and negative leader during the attachment process is also examined [Lu et al., 2015], showing systematic acceleration of upward connecting leader as the downward leader approaches the ground.

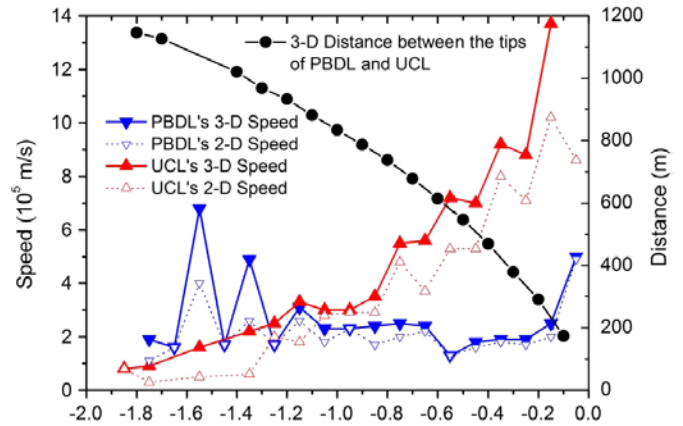


Fig. 9. 3-D and 2-D propagation characteristics of the PBDL and the UCL in F1215 versus time. The solid lines with solid symbols show the 3-D characteristics, and the dot lines with hollow symbols show the 2-D characteristics. [Adopted from Gao et al., 2014]

### C. New insight into unique CG lightning discharges

Two bi-polar CG lightning flashes were recorded on high-speed video cameras with concurrent electromagnetic measurements and optical observations, both containing one leading positive CG stroke followed by multiple negative CG strokes [Chen et al., 2015a; Tian et al., 2016]. The velocity of return strokes and the preceding downward leaders (of positive and negative polarity, respectively) in a bi-polar CG flash terminated on a 90 m tall building was estimated for the first time [Chen et al., 2015]. The characteristics of optimal pulses from the positive and negative return strokes in the bipolar flash are presented. By referring to concurrent radar observations of thunderstorm reflectivity, the conceptual charge structure of parent thunderstorm is also proposed [Tian et al., 2016], indicating that the occurrence of subsequent negative CG strokes is closely associated with the positive leader propagating into the laterally displaced negative cloud region near the cloud base.

A multiple termination CG flash with four stepped leader-stroke sequences are well mapped by the LMI (Fig. 10). The four stepped leader-stroke sequences were produced from two different branches of the preliminary breakdown process inside the cloud, and the time intervals between each adjacent two leader-stroke sequences were 82.9 ms, 81.4 ms, and 152.2 ms, respectively. The first two stroke sequences were multiple termination strokes (MTSs), and each MTS showed two different ground terminations induced by two leader branches [Sun et al., 2016]. Based on LMI and high speed video observation, two mechanisms for multiple-ground terminations

are revealed (Jiang et al, 2015; Sun et al, 2016): (1) different incloud preliminary breakdown branches propagate outside the cloud and contact ground with different channels; (2) different stepped-leader branches sharing same incloud and upper main channel contact ground in sequence [Sun et al., 2016].

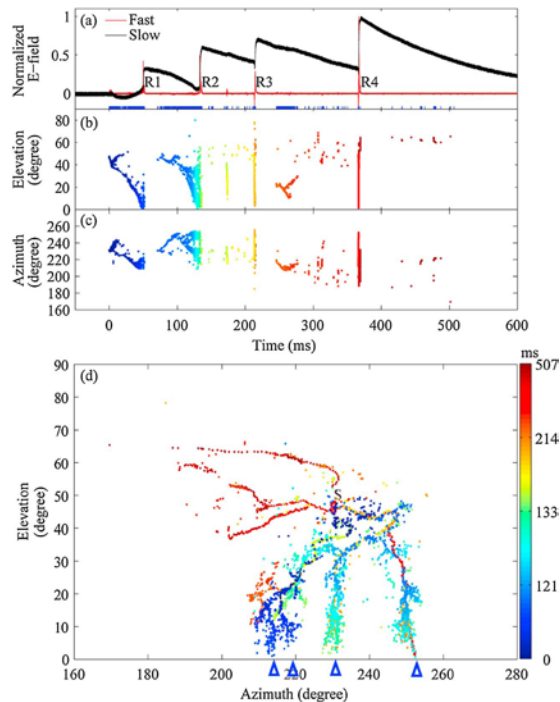


Fig. 10. Progression of a lightning flash with multiple-ground terminations mapped by the lightning VHF radiation location system with time resolution of 1 microsecond. [Adopted from Sun et al., 2016]

#### D. Propagation of lightning-radiated electromagnetic field

The propagation effect of the lightning-radiated electromagnetic field along the ground surface is very important for lightning detection and location and so on. The propagation characteristics of lightning electromagnetic field has been widely studied, in terms of along a lossy ground with inhomogeneous path (stratified and mixed path) and frequency dependent earth parameters [Zhang et al., 2014b] and rough ground surface [Li et al., 2014], and the effect of striking tall objects on the field-to-current conversion factors [Zhang et al., 2014a, 2014c]. Recently, A theoretical analysis of the propagation effects of lightning electromagnetic fields over a mountainous terrain is presented [Li et al., 2016b], which is supported by experimental observations consisting of simultaneous records of lightning currents and electric fields associated with upward negative lightning flashes to the instrumented Santis tower in Switzerland, and found that considering the real irregular terrain between the Santis tower and the field measurement station, both the shape of waveform and amplitude of the simulated electric fields associated with return strokes and fast initial continuous current pulses are in excellent agreement with the measured waveforms, however, the assumption of a flat ground results in a significant under estimation of the peak electric field.

Further, we have analyzed the propagation effects on lightning-radiated electromagnetic fields over mountainous

terrain by using a 3-D FDTD method [Li et al., 2016a], and discussed the time delay error in the time-of-arrival (TOA) technique currently used to locate lightning in detection networks, it is found that the time delays and amplitudes of the lightning-radiated electromagnetic fields can be significantly affected by the presence of a mountainous terrain and the time delay resulting from the finite ground conductivity appears to be smaller than that caused by the mountainous terrain, and we should consider the effect of the a mountainous terrain on the lightning location accuracy in the future.

#### E. Lightning hazard causes and protection technique testing

At both triggered lightning experiment sites located in Shandong and Guangdong, we have set up better measurement infrastructure (that contains multi-disciplinary instrumentations and numerical modeling techniques) to study lightning physics and also the platform to test the lightning hazards (to power transmission lines, telecommunication devices, and power systems, etc) and the performance of lightning protection techniques (such as surge protection devices). It is desired that, through the comprehensive experiments based on these platforms, we can improve the capability to reduce the damage and economic loss caused by lightning hazards.

As one of the experiments, we investigated the performance of grounding system in the lightning protection technique and the ground potential rise due to the nearby lightning strokes [Chen et al., 2015b; Liu et al., 2015]. In particular, the current numerical modeling effort has been made to evaluate the mechanism for the ionization of soil (for four different types) under the impact of lightning strike, which provides more thoughts on the relevant field experiment.

#### REFERENCES

- Chen, L., W. Lu, Y. Zhang, D. Wang, (2015a), Optical Progression Characteristics of an Interesting Natural Downward Bipolar Lightning Flash, *Journal of Geophysical Research-Atmospheres*, 120, doi:10.1002/2014JD022463.
- Chen, S., Y. Zhang, C. Chen, X. Yan, W. Lu, Y. Zhang (2015b), Influence of the Ground Potential Rise on the Residual Voltage of Low-Voltage Surge Protective Devices due to Nearby Lightning Flashes, *IEEE Trans. on Power Delivery*, doi: 10.1109/TPWRD.2015.2441773.
- Gao, Y., W. Lu, Y. Ma, L. Chen, Y. Zhang, Y. Xu, and Y. Zhang (2014), Three-dimensional propagation characteristics of the upward connecting leaders in six negative tall-object flashes in Guangzhou, *Atmos. Res.*, 149, 193-203.
- Jiang, R., Z. Wu, X. Qie, D. Wang, and M. Liu (2014a), High-speed video evidence of a dart leader with bidirectional development. *Geophys. Res. Lett.*, 41, doi: 10.1002/2014GL060585.
- Jiang, R. B., X. S. Qie, Z. J. Wu, D. F. Wang, M. Y. Liu, G. P. Lu, and D. X. Liu (2014b), Characteristics of upward lightning from a 325-m-tall meteorology tower. *Atmos. Res.*, 149, 111-119. doi: 10.1016/j.atmosres.2014.06.007.
- Jiang, R., X. Qie, Z. Wang, H. Zhang, G. Lu, Z. Sun, M. Liu, and X. Li (2015), Characteristics of lightning leader propagation and ground attachment, *J. Geophys. Res. Atmos.*, 120, doi:10.1002/2015JD023519.
- Kong, X., Y. Zhao, T. Zhang (2005), Optical and electrical characteristics of in-cloud discharge activity and downward leaders in positive cloud-to-ground lightning flashes, 160: 28-38
- Li D., Zhang, Q., et al., (2014). Computation of Lightning Horizontal Field Over the Two-Dimensional Rough Ground by Using the Three-Dimensional FDTD, VOL. 56, NO. 1, FEBRUARY 2014
- Li, D., M. Azadifar, F. Rachidi, M. Rubinstein, G. Diendorfer, K. Sheshyekani, Q. Zhang, and Z. Wang (2016a), Analysis of lightning electromagnetic field propagation in mountainous terrain and its effects on ToA-based

- lightning location systems, *J. Geophys. Res. Atmos.*, 121, 895–911, doi:10.1002/2015JD024234.
- Li, D., M. Azadifar, F. Rachidi, M. Rubinstein, G. Diendorfer, K. Sheshyekani, Q. Zhang, and Z. Wang (2016b), On Lightning Electromagnetic Field Propagation Along an Irregular Terrain *IEEE Trans. Electromagn. Compat.*, 58(1): 161
- Li W., X. Qie, S. Fu, Y. Shen (2016), Simulation of Quasi-Linear Mesoscale Convective Systems in Northern China: Lightning Activities and Storm Structure. *Adv. Atmos. Sci.*, 33(1): 85-100.
- Liu, K., X. Qie, J. He, G. Lu, and Q. Xia (2015), Estimation of critical electric field of soil ionization based on tangential electric field method, *IET Sci. Meas. Technol.*, 9(6), doi: 10.1049/iet-smt.2014.0352.
- Liu, D. X., X. S. Qie, L. Peng, and W. L. Li, 2014: Charge structure of a summer thunderstorm in North China: Simulation using a regional atmospheric model system. *Adv. Atmos. Sci.*, 31, 1022–1034, doi: 10.1007/s00376-014-3078-7.
- Lu, G., R. Jiang, X. Qie, H. Zhang, Z. Sun, M. Liu, Z. Wang, and K. Liu (2014), Burst of intracloud current pulses during the initial continuous current of a rocket-triggered lightning flash, *Geophys. Res. Lett.*, 41, doi: 10.1002/2014GL062127.
- Lu, W., L. Chen, Y. Ma, V. A. Rakov, Y. Gao, Y. Zhang, Q. Yin, and Y. Zhang (2013), Lightning attachment process involving connection of the downward negative leader to the lateral surface of the upward connecting leader, *Geophys. Res. Lett.*, 40, 5531–5535, doi:10.1002/2013GL058060.
- Lu, W., Y. Gao, L. Chen, Q. Qi, Y. Ma, Y. Zhang, S. Chen, X. Yan, C. Chen, and Y. Zhang (2015), Three-dimensional propagation characteristics of the leaders in the attachment process of a downward negative lightning flash, *J. Atmos. Sol. Terr. Phys.*, 136, 23-30, doi:10.1016/j.jastp.2015.07.011
- Qie, X.S., R.P. Zhu, T. Yuan, X.K. Wu, W. L. Li, and D.X. Liu, 2014: Application of total-lightning data assimilation in a mesoscale convective system based on the WRF model. *Atmospheric Research*, 145–146: 255–266, 10.1016/j.atmosres.2014.04.012
- Sun, Z., X. Qie, M. Liu, R. Jiang, Z. Wang, and H. Zhang (2016), Characteristics of a negative lightning with multiple-ground terminations observed by a VHF lightning location system, *J. Geophys. Res. Atmos.*, 121, doi:10.1002/2015JD023702.
- Sun, Z., X. Qie, R. Jiang, M. Liu, X. Wu, Z. Wang, G. Lu, and H. Zhang (2014), Characteristics of a rocket-triggered lightning flash with large stroke number and the associated leader propagation, *J. Geophys. Res. Atmos.*, 119(23):13,388–13,399. doi:10.1002/2014JD022100.
- Sun, Z., X. Qie, M. Liu, R. Jiang, Z. Wang, and H. Zhang (2016), Characteristics of a negative lightning with multiple-ground terminations observed by a VHF lightning location system, *J. Geophys. Res. Atmos.*, 121, doi:10.1002/2015JD023702.
- Tan, Y., Z. Liang, Z. Shi, J. Zhu, and X. Guo (2014a), Numerical simulation of the effect of lower positive charge region in thunderstorms on different types of lightning. *Sci. China (Earth Sciences)*, 57, 2125-2134
- Tan, Y., S. Tao, Z. Liang, and B. Zhu (2014b), Numerical study on relationship between lightning types and distribution of space charge and electric potential, *J. Geophys. Res. Atmos.*, 119, 1003–1014, doi:10.1002/2013JD019983.
- Tian, Y., X. Qie, G. Lu, R. Jiang, Z. Wang, H. Zhang, M. Liu, Z. Sun and G. Feng (2016), Characteristics of a bipolar cloud-to-ground lightning flash containing a positive stroke followed by three negative strokes, 10.1016/j.atmosres.2016.02.023. (in press)
- Wang, F., Y. Zhang, D. Zheng (2015), Impact of the vertical velocity field on charging processes and charge separation in a simulated thunderstorm, *J. Meteor. Res.*, 29(2):328-343
- Wang, Y., X. Qie, D. Wang, M. Liu (2016). Beijing Lightning Network (BLNET): A research and operational system for comprehensive lightning detection, *Atmos. Res.*, 171:121-132
- Wang, Y., Y. Yang, and C. Wang, (2014), Improving forecasting of strong convection by assimilating cloud-to-ground lightning data using the physical initialization method, *Atmos. Res.*, 150, 31-41
- Xu, L., Y. Zhang, H. Liu, D. Zheng, F. Wang (2016), The Role of Dynamic Transport in the Formation of the Inverted Charge Structure in a Simulated Hailstorm, *Sci. China (Earth Sciences)* (in press).
- Zhang, Q., L. He, T. Ji, and W. Hou (2014a), On the field-to-current conversion factors for lightning strike to tall objects considering the finitely conducting ground, *J. Geophys. Res. Atmos.*, 119, 8189–8200, doi:10.1002/2014JD021496
- Zhang, Q., T. Ji, W. Hou, et al., (2014b). Effect of Frequency Dependent Soil on the Propagation of Electromagnetic Fields Radiated by Subsequent Lightning Strike to Tall Towers, *IEEE Trans. Electromagn. Compat.*, Accepted (SCI)
- Zhang, Q., W. Hou, T. Ji, L. He, (2014c). Validation of Far-Field-Current Relationship for the Lightning Strike to Electrically Short Objects, *Journal of Atmospheric and Solar-Terrestrial Physics*, <http://dx.doi.org/10.1016/j.jastp.2014.08.015>
- Zhao, P., Y. Yin, and H. Xiao (2015), The effects of aerosol on development of thunderstorm electrification: A numerical study, *Atmos. Res.*, 153, 376-391